inorganics

MDPI

Article

Investigating the Influence of Various Inorganic Fillers on Thermal, Fire Performance, and Mechanical Properties of Polylactic Acid

Ntombizanele Jafta [1], Mpho Phillip Motloung [2,*], Ntsoaki Joyce Malebo [1] and Mokgaotsa Jonas Mochane [2,*]

[1] Department of Life Sciences, Central University of Technology, Private Bag X20539, Bloemfontein 9301, South Africa; njafta@cut.ac.za (N.J.); nmalebo@cut.ac.za (N.J.M.)
[2] Department of Chemistry, College of Science, Engineering and Technology, University of South Africa, Florida Science Campus, Johannesburg 1710, South Africa
* Correspondence: motlomp1@unisa.ac.za (M.P.M.); mochamj@unisa.ac.za (M.J.M.)

Abstract

This study investigated the influence of zinc oxide (ZnO), titanium dioxide (TiO_2), and calcium carbonate ($CaCO_3$) on the material properties of PLA processed by melt compounding in a twin-screw extruder. The results demonstrated that the incorporation of ZnO and $CaCO_3$ reduced the thermal stability of PLA. Furthermore, ZnO reduced the complex viscosity and tensile strength of PLA. In contrast, the addition of TiO_2 maintained the thermal stability, complex viscosity, and mechanical properties of PLA. Moreover, it was observed that combining ZnO with TiO_2 and $CaCO_3$ preserved the mechanical properties of PLA. The findings underscore the significance of hybridization, as it enhanced the properties of PLA/ZnO nanocomposites. Among all the developed composites, ZnO/TiO_2 demonstrated better performance, which could be attributed to the finer dispersion of the fillers observed by scanning electron microscopy. Overall, the findings demonstrate the potential of maintaining the properties of PLA in PLA/ZnO composites through the hybridization of inorganic fillers, particularly when prepared using melt processing.

Keywords: polylactic acid; zinc oxide; thermal stability; inorganic filler

1. Introduction

Polylactic acid (PLA) is a commercially produced thermoplastic biopolymer and represents a viable substitute for petroleum-based polymers across different industrial sectors. PLA is widely used in applications such as textiles, biomedical, and packaging [1]. Nevertheless, PLA's use in biomedical and food packaging is limited by its lack of functional properties, such as antimicrobial and antioxidant activity. Consequently, PLA is commonly blended with materials that exhibit these functional properties. Typical examples include blending PLA with metal nanoparticles and metal oxides [2–4]. Metal oxides nanoparticles, such as zinc oxide (ZnO), have been widely used in the development of functional PLA-based composites for potential applications in food packaging and biomedical fields. ZnO can be synthesized using various methods, which can produce different morphologies suitable for a wide range of applications. It is generally considered non-toxic and exhibits chemical stability, high catalytic activity, and antibacterial properties. ZnO is widely used in cosmetics, photocatalytic degradation, agriculture, food packaging, and biomedical applications [5,6]. Kim et al. [4] developed PLA/ZnO composites for potential use in food packaging. The developed composites exhibited antibacterial activity against *Staphylococcus aureus* (*S. aureus*) and *Escherichia coli* (*E. coli*), which increased with increasing ZnO

Check for updates

Academic Editor: Kenneth J.D. MacKenzie

Received: 1 July 2026
Revised: 5 November 2026
Accepted: 8 November 2026
Published: 12 November 2026

Copyright: © 2026 by the authors. Licensee MDPI, Basel, Switzerland. This article is an open access article distributed under the terms and conditions of the Creative Commons Attribution (CC BY) license.

concentration, demonstrating the efficacy of this metal oxide for developing active food packaging materials. Salaris et al. [7] developed electrospun PLA-based nanofibers containing 0.5–20 wt.% ZnO. An optimum ZnO loading of 3 wt.% was identified, resulting in improved mechanical and thermal properties. For example, although the mechanical properties of the composites decreased compared with those of neat PLA, the highest tensile strength, elongation at break, and elastic modulus were obtained at a concentration of 3 wt.% compared with the other concentrations.

Although ZnO imparts functional properties when incorporated into PLA, its use presents certain limitations, particularly during melt compounding. Melt processing is a widely employed technique for the large-scale production of polymer composites. However, producing PLA/ZnO composites using melt processing methods presents a significant challenge, as ZnO can promote degradation of the PLA matrix. During melt processing, PLA degradation is often reflected in reduced thermal stability and complex viscosity, potentially indicating a reduction in molecular weight. For instance, the average molecular weight of PLA decreased by 55% when incorporating 1.5 wt.% ZnO [8]. Morici et al. [9] observed a reduction in PLA complex viscosity as ZnO concentration increased from 0.5 to 2 wt.%. Frequency sweep tests can be used to evaluate thermal degradation of biopolymers by monitoring the evolution of complex viscosity as a function of angular frequency [10]. Kim et al. [4] also reported a significant reduction in the thermal stability of PLA with increasing ZnO concentration, highlighting the need to enhance the processing stability of PLA/ZnO, considering the multiple steps, including compounding to prepare composites, followed by processes such as injection molding or film blowing. A reduction in complex viscosity may indicate a decrease in polymer molecular weight, although viscosity can be influenced by other factors. Similarly, the reduction in thermal stability may indicate polymer degradation and can be accompanied by a reduction in mechanical properties.

Titanium dioxide (TiO_2) is an inorganic metal oxide filler that exhibits antioxidant and antimicrobial properties under suitable conditions, and photocatalytic activity. It is also widely used because of its UV-absorption capabilities [11]. Unlike ZnO, the incorporation of TiO_2 into PLA does not appear to induce chain scission and reduction in viscosity under the conditions investigated by Morici et al. [9]. Additionally, TiO_2 can impart antibacterial functionality to PLA. For example, 0.75 wt.% TiO_2 could improve antibacterial activity against *E. coli* and *S. aureus* by 1115 and 1268%, compared to neat PLA fibers [12]. Previous studies have reported an optimum TiO_2 loading of approximately 3 wt.% in PLA [13,14]. For example, Zhuang et al. [13] demonstrated that incorporating 3 wt.% modified TiO_2 significantly improved the tensile strength, elongation at break, and Young's modulus of PLA. However, these properties declined substantially at higher TiO_2 concentrations. At higher concentrations, nanofillers tend to agglomerate and cause a reduction in mechanical properties.

Calcium carbonate ($CaCO_3$) is another effective filler for improving the performance of PLA. It is widely used in polymer formulations because of its low toxicity, cost-effectiveness, and ability to modify mechanical properties [15,16]. In addition, $CaCO_3$ can improve brightness and gloss in polymers. At the nanoscale, $CaCO_3$ can influence complex viscosity, enhance mechanical properties, and reduce the shrinkage of polymer nanocomposites [17,18]. Oksuz and Yildirim [19] investigated the effects of $CaCO_3$ loading concentrations ranging from 3 to 15 wt.% on the properties of PP/EVA composites. The optimum loading was 3 wt.%, which resulted in considerable improvements in elastic modulus, impact strength, and thermal properties. Collectively, these studies [7,13,14,19] suggest that a filler loading of approximately 3 wt.% can be beneficial under certain conditions. However, ZnO has also been reported to adversely affect the properties of PLA/ZnO composites. To address this limitation, the simultaneous incorporation of ZnO with TiO_2 or $CaCO_3$ may help mitigate these adverse effects while maintaining the properties of PLA.

Hybrid filler systems have attracted considerable attention due to the complementary properties contributed by individual fillers. Tajdari et al. [20] developed PLA hybrid composites containing ZnO/TiO_2 by using the solution casting method. Their study provided insights into the effects of incorporating these metal oxides simultaneously on the properties of PLA. However, the solution casting method limits the extent to which the findings can be extrapolated to melt processing conditions, where there are effects of shear stress and elevated temperatures. Furthermore, studies investigating the combined incorporation of ZnO and CaCO3 into PLA remain limited. Nevertheless, the incorporation of nano-ZnO/$CaCO_3$ into natural rubber has been reported to improve its mechanical properties [21]. Therefore, this finding provides rationale for investigating whether these fillers can produce synergistic effects when incorporated into PLA.

Combining ZnO with TiO_2 and $CaCO_3$ may offer a promising strategy for balancing the processing stability and functional properties of PLA-based composites. Therefore, this study investigates the effects of incorporating TiO_2 and $CaCO_3$ individually in combination with ZnO on the properties of PLA/ZnO composites. The total filler concentration was maintained at 3 wt.% for each hybrid formulation, based on findings reported in previous studies [7,13,14,19]. TiO_2 and $CaCO_3$ were incorporated at equal amounts relative to ZnO, with the aim of mitigating processing-induced degradation and reductions in thermal stability of PLA, while maintaining balanced mechanical performance. It is worth mentioning that these inorganic fillers were used without any surface modification or treatment. In addition, the coupling agents were not introduced because the study is designed to evaluate the effects of the fillers without introducing additional variables. To the best of our knowledge, a systematic approach investigating $CaCO_3$/ZnO and TiO_2/ZnO hybrid filler systems in PLA, with particular emphasis on rheological behavior, processing stability, and the balance of material properties, has not been previously reported.

2. Results and Discussion

2.1. Morphology

Figure 1 illustrates the SEM micrographs of the investigated samples. PLA/ZnO nanocomposites revealed a distribution of ZnO nanoparticles, with some obvious aggregates within the matrix (Figure 1a). Taha et al. [22] observed a rougher surface at 3 wt.% ZnO nanoparticles, which appeared embedded in the PLA matrix. TiO_2 appeared finely dispersed with fewer aggregates, as illustrated in Figure 1b. The $CaCO_3$ particles are evenly distributed within the PLA matrix, although there are some obvious interfacial gaps between particles and the matrix (Figure 1c). The incorporation of the two metal oxides resulted in finer dispersion of the nanoparticles, which also appear embedded within the PLA matrix (Figure 1d). Some reported studies showed a tendency of forming the aggregates upon simultaneous incorporation of ZnO and TiO_2 into PLA [20]. On the other hand, the ZnO/$CaCO_3$ composite system was characterized by obvious spherical particles on the surface, which could be attributed to $CaCO_3$ (Figure 1e). Overall, single-filler composites demonstrated better distribution and dispersion of the incorporated fillers, although the $CaCO_3$ showed more agglomerates with clear interfacial gaps. However, the hybrid metal-oxide-based systems showed finer dispersion, with both fillers embedded within the matrix.

2.2. Thermal Properties

2.2.1. Thermal Stability

The TGA curves of the prepared composites are presented in Figure 2. The maximum degradation temperature (T_{max}) and early degradation temperature taken at 10% weight loss ($T_{10\%}$) are summarized in Table 1. ZnO decreased the thermal stability of PLA, whereas TiO_2

maintained its thermal stability. A reduction in the thermal stability of PLA in the presence of ZnO has also been reported [7,23]. ZnO has been reported to catalyze transesterification or unzipping depolymerization through coordination with the carbonyl groups of polymer chains, consequently reducing the thermal stability of PLA. Wang et al. [23] observed a stronger catalytic effect of ZnO nanoparticles on reducing the thermal stability of PLA than TiO_2. $CaCO_3$ also decreased the thermal stability of PLA; however, the thermal stability of the $CaCO_3$-based composite was higher than that of the ZnO-based composite. This reduction in thermal stability may be attributed to the basic catalytic nature of $CaCO_3$, which can promote the depolymerization of PLA through its ester bonds [24].

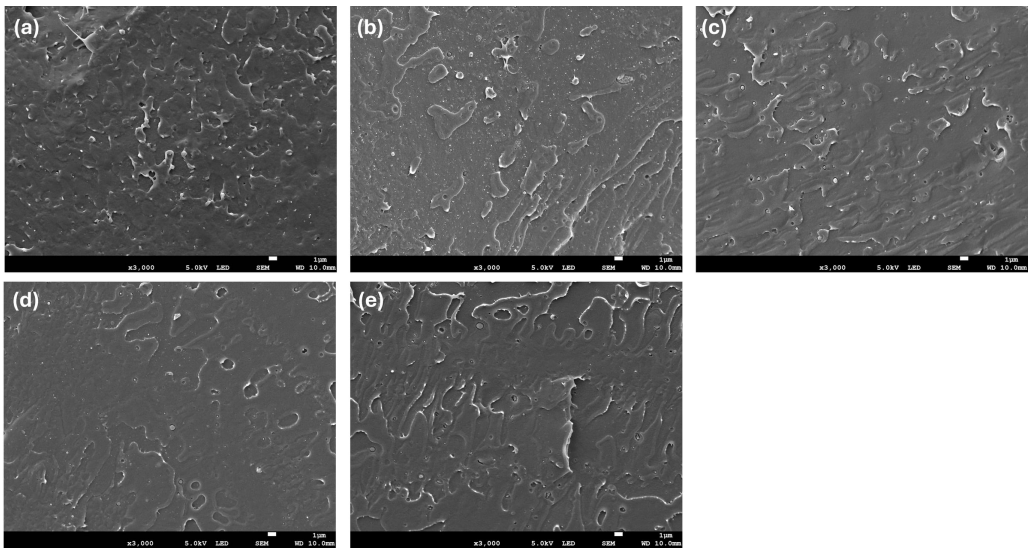


Figure 1. SEM micrographs of (**a**) PLA/ZnO, (**b**) PLA/TiO_2, (**c**) PLA/$CaCO_3$, (**d**) PLA/ZnO/TiO_2, and (**e**) PLA/ZnO/$CaCO_3$.

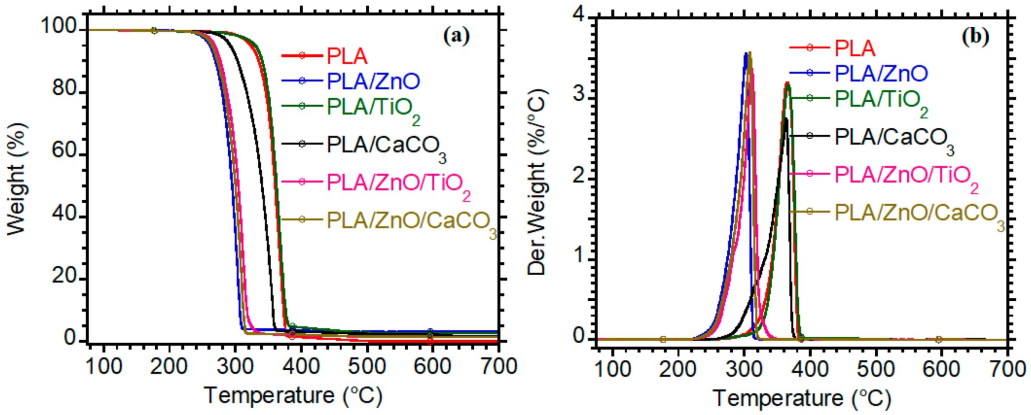


Figure 2. (**a**) TGA curves and (**b**) derivative curves of the prepared samples.

All ZnO-containing hybrid nanocomposites showed lower thermal stability than neat PLA, with degradation temperatures within the range observed for PLA/ZnO composites. ZnO can reduce polymer thermal stability through catalytic degradation; however, at very low concentrations (up to 0.15%), it can also shift degradation temperatures to higher values [15]. The observed reduction in thermal stability of PLA may indicate that ZnO catalyzed the early degradation of the polymer matrix, potentially promoting the release of volatile degradation products. This effect may have counteracted the ability of TiO_2 to maintain the thermal stability of PLA. The ZnO/TiO_2 and ZnO/$CaCO_3$ hybrid filler systems did not exhibit significant improvements compared to the PLA/ZnO system, which

suggests that the catalytic degradation effect of ZnO may have dominated the behavior of the hybrid filler systems. Shojaeiarani et al. [8] investigated the molecular weight and melt flow index (MFI) of PLA composites containing ZnO at concentrations varying from 0.5 to 1.5 wt.%. The authors reported a significant reduction in the average molecular weight and a substantial increase in the MFI of PLA. Although molecular weight and MFI were not determined in the present study, these findings may suggest that ZnO may promote polymer chain scission, which can reduce the molecular weight of PLA and increase its melt flow.

Table 1. Summarized cone calorimeter parameters (PHRR and THR) and the TGA results.

Sample	$T_{10\%}$	T_{max} (°C)	PHRR ($kW \cdot m^{-2}$)	THR ($MJ \cdot m^{-2}$)
PLA	337.2	363.2	359.2	67.4
PLA/ZnO	269.4	300.6	490.1	68.9
PLA/TiO_2	340.6	366.7	344.9	68.1
PLA/$CaCO_3$	303.8	364.9	417.2	73.9
PLA/ZnO/TiO_2	276.1	311.1	524.7	92.9
PLA/ZnO/$CaCO_3$	272.2	307.6	581.4	79.6

2.2.2. DSC Thermal Properties

Figure 3 illustrates the influence of ZnO, TiO_2, and $CaCO_3$ on the thermal properties of PLA, determined by DSC. The cooling curves are presented in Figure 3a and show only the glass transition temperature (T_g) of PLA at approximately 60 °C. PLA is characterized by a relatively slow crystallization rate; hence, no crystallization temperature was observed during cooling, particularly at the cooling rate of 10 °C/min used in this study. As summarized in Table 2, no significant differences in T_g were observed among the prepared samples. Figure 3b depicts the second heating curves, in which the T_g remains apparent at approximately 60 °C. Cold crystallization temperature (T_{cc}) is observed at a temperature of 110.8 °C for neat PLA, followed by a melt–recrystallization–melt phenomenon, which is characteristic of PLA [25,26]. The addition of ZnO shifted the T_{cc} to a higher temperature of 123.3 °C, suggesting that ZnO delayed the cold crystallization of PLA during heating. The melting temperatures remained similar to those of neat PLA, indicating a limited effect on the melting behavior of PLA. Shankar et al. [27] reported that the addition of ZnO (0.5–1.5 wt.%) to PLA did not significantly affect its T_g, T_{cc}, or melting temperature (T_m). Similarly, Salaris et al. [7] observed that the T_g of PLA remained within a similar range following the incorporation of ZnO, whereas T_{cc} shifted significantly to higher temperatures. The incorporation of TiO_2 and $CaCO_3$ as individual fillers did not significantly affect the thermal transitions of PLA. However, the ZnO/TiO_2-based composites exhibited an increase in T_{cc} to 117.1 °C, which may be associated with delayed crystallization behavior in the presence of ZnO nanoparticles. The calculated crystallinity of the prepared samples is also summarized in Table 3. PLA showed crystallinity of 2.8%, which slightly shifted to 4.3% when incorporating ZnO. The ZnO/TiO_2 hybrid system had crystallinity of 6.6%, which was the highest compared to neat PLA and other composites. This could be attributed to homogeneous dispersion of these metal oxides, which promoted nucleation and subsequent increase in crystallinity.

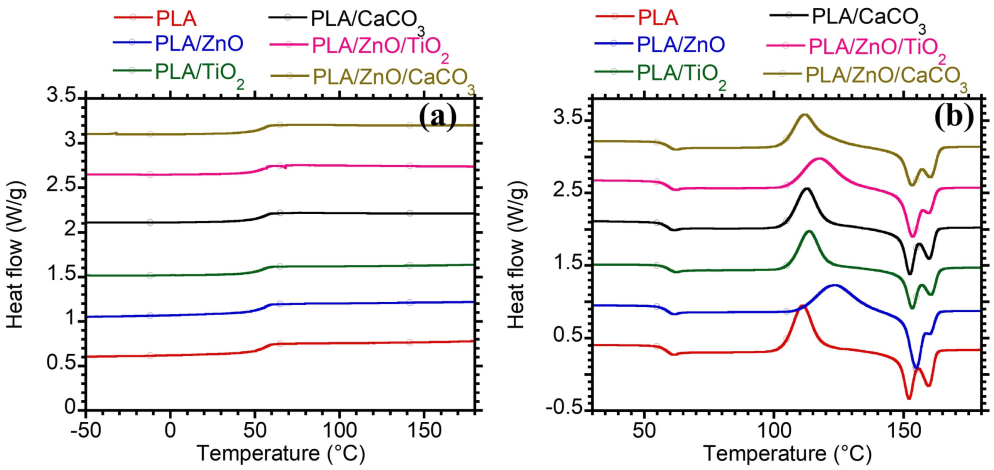


Figure 3. (**a**) DSC cooling curves and (**b**) second heating curves.

Table 2. Summarized DSC thermal transitions.

Sample	T_g (°C)	T_{cc} (°C)	T_{m1} (°C)	T_{m2} (°C)	X_c
PLA	57.9	110.8	151.6	159.2	2.8
PLA/ZnO	58.1	123.3	154.6	160.8	4.3
PLA/TiO_2	58.3	113.3	152.9	160.4	2.4
PLA/$CaCO_3$	58.7	112.5	152.1	160.0	3.9
PLA/ZnO/TiO_2	57.9	117.1	153.3	159.2	6.6
PLA/ZnO/$CaCO_3$	57.5	113.3	152.9	160.4	1.5

Table 3. Summarized tensile properties and impact resistance values.

Sample	Tensile Strength (MPa)	Tensile Modulus (MPa)	Elongation at Break (%)	Impact Resistance ($kJ \cdot m^{-2}$)
PLA	59.8 ± 2.2	1925.5 ± 83	4.1 ± 0.1	5.6 ± 0.3
PLA/ZnO	53.7 ± 10.8	1906.7 ± 75.9	3.7 ± 0.7	5.6 ± 0.3
PLA/TiO_2	58.5 ± 2.7	1878.9 ± 59.1	5.7 ± 0.6	5.9 ± 0.2
PLA/$CaCO_3$	58.4 ± 1.1	1922.7 ± 50.5	5.6 ± 1.2	5.9 ± 0.5
PLA/ZnO/TiO_2	58.9 ± 10.3	1996.8 ± 28.6	5.3 ± 1.7	5.5 ± 0.7
PLA/ZnO/$CaCO_3$	60.0 ± 3.4	1842.7 ± 112.8	5.6 ± 1.5	5.7 ± 0.2

2.3. Rheological Properties

Figure 4 presents the complex viscosity against the angular frequency for all the prepared samples. Neat PLA exhibited Newtonian behavior at low frequencies, followed by shear-thinning behavior at higher frequencies. This behavior is typical for homopolymer PLA. Upon the addition of ZnO, the complex viscosity decreased substantially, accompanied by pronounced shear-thinning behavior at low angular frequencies. This behavior is primarily attributed to ZnO-induced chain scission during melt processing. Similar behavior has been reported, with the addition of 2 wt.% ZnO resulting in a significant reduction in viscosity of PLA [7]. In contrast, the incorporation of TiO_2 and $CaCO_3$ individually maintained a complex viscosity similar to that of neat PLA. The hybrid filler systems exhibited substantially lower complex viscosity than neat PLA. This reduction may be associated

with the presence of ZnO, which could promote polymer chain scission and consequently decrease the molecular weight and viscosity of the PLA matrix.

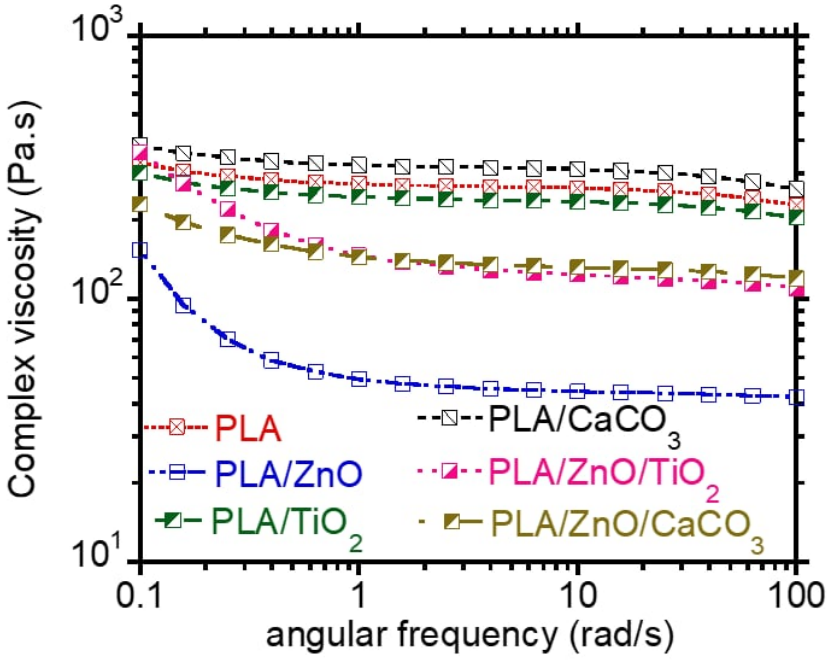


Figure 4. Complex viscosity curves of the prepared samples.

2.4. Mechanical Properties

Table 3 summarizes the tensile and Charpy impact properties of neat PLA and PLA-based nanocomposites. Neat PLA exhibited a tensile strength of 59.8 ± 2.2 MPa, which decreased by approximately 10% to 53.7 ± 10.8 MPa upon the addition of 3 wt.% ZnO. This reduction may be due to ZnO-induced chain scission during melt processing, potentially reducing the material's ability to withstand and distribute the mechanical stress. In contrast, the incorporation of $CaCO_3$ and TiO_2 individually into PLA maintained the tensile strength of PLA. The ZnO/TiO_2 and $ZnO/CaCO_3$ hybrid systems also maintained the tensile strength comparable to that of neat PLA, as shown in Table 3. The tensile modulus decreased upon the incorporation of ZnO and TiO_2, whereas that of the $PLA/CaCO_3$ composite remained comparable to that of neat PLA. The highest tensile modulus was obtained for the ZnO/TiO_2 hybrid system, reaching 1996.8 MPa. This could be attributed to reinforcing effect of crystals formed in this system.

A slight reduction in elongation at break from 4.1% to 3.7% was also noticed upon addition of ZnO. The other nanocomposites showed slightly higher elongation at break values. Incorporating ZnO and TiO_2 at equal amounts (i.e., 1.5 wt.% each) maintained the tensile strength of PLA, while slightly increasing its elongation at break and tensile modulus. These improvements may be associated with the reinforcing effect of TiO_2 and the combined effects of the two fillers. The ZnO/TiO_2 showed better dispersion of the metal oxide nanoparticles with fewer agglomerates, which may have contributed to the observed improvements in tensile modulus and elongation at break relative to neat PLA and the PLA/ZnO composite. Similarly, the simultaneous incorporation of ZnO and $CaCO_3$ maintained the tensile strength of PLA and slightly increased the elongation at break, although the tensile modulus decreased to 1842.7 MPa.

The observed findings indicate that combining ZnO with TiO_2 or $CaCO_3$ helps preserve the tensile strength of PLA compared with the reduction observed upon incorporating ZnO alone. These findings demonstrate the potential benefits of combining inorganic fillers to

tailor the mechanical properties of PLA. This shows that hybridization of ZnO with these nanofillers at equal amounts provides an effective strategy for maintaining the mechanical properties of PLA. However, future research work should investigate whether these effects arise from synergistic interaction of these inorganic fillers at lower concentrations (e.g., 0.5 wt.% each). Furthermore, the effect of loading concentration should also be investigated. The Charpy impact properties are summarized in Table 3. Neat PLA is brittle, and it exhibits relatively low impact strength. The incorporation of the inorganic fillers did not significantly affect the impact strength of PLA, implying the incorporated filler did not alter its resistance to fracture.

2.5. Flammability Properties

Figure 5a,b illustrates the heat release rate (HRR) and total heat release (THR) curves of the prepared composites, providing insights into the effects of different inorganic fillers on the flammability behavior of PLA. The peak heat release rate (PHRR) and THR values are summarized in Table 1. Neat PLA exhibited PHRR and THR values of 359.2 kW·m^{-2} and 67.4 MJ·m^{-2}, respectively. Upon the incorporation of ZnO, the PHRR increased to 490.1 kW/m^2, indicating that ZnO worsened the flammability of PLA. THR, however, did not show any significant difference compared to neat PLA. The TGA results showed a reduction in the thermal stability of PLA when adding ZnO, suggesting that ZnO may catalyze thermal degradation of PLA and potentially accelerate the release of combustible volatile products that further support combustion. The increased PHRR may indicate that the ZnO-containing composite was less effective at forming a protective layer on the surface of PLA.

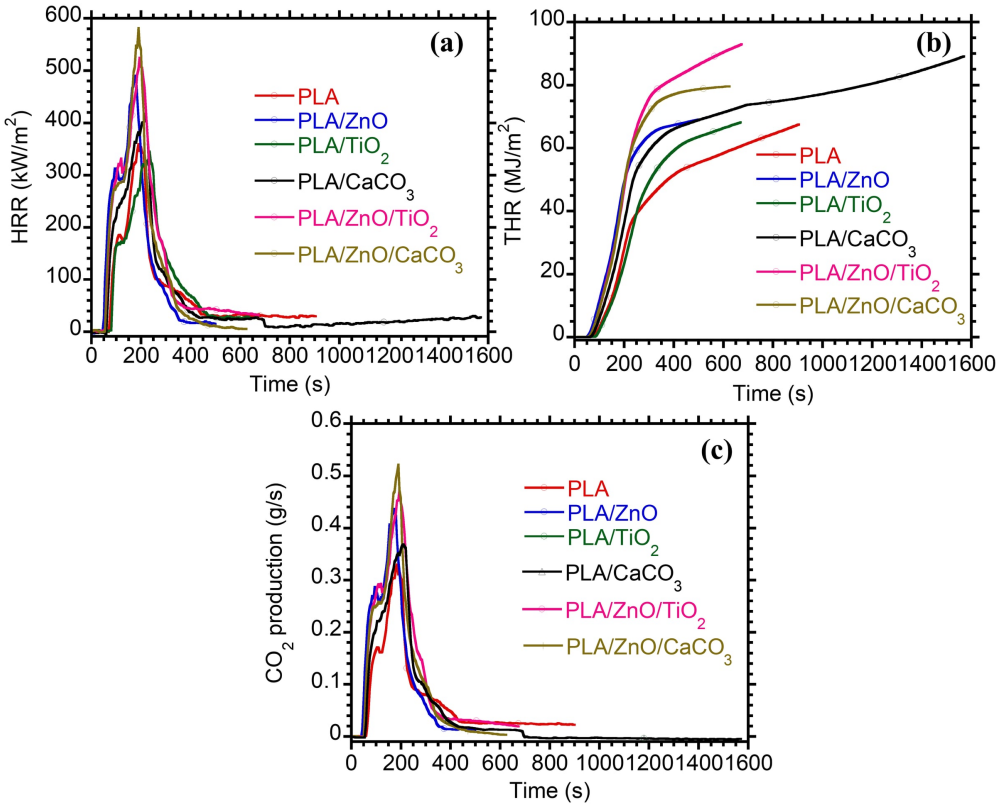


Figure 5. Cone calorimeter plots. (**a**) HRR, (**b**) THR, and (**c**) CO_2 production.

PLA/$CaCO_3$ composite exhibited a similar reduction in thermal stability to the PLA/ZnO composite, although its PHRR was less than that of PLA/ZnO. In contrast,

the PLA/TiO_2 nanocomposite exhibited a PHRR of 344.9 kW·m^{-2} and THR of 68.1 MJ·m^{-2}, which was in the same range as neat PLA, indicating limited effect on the heat release behavior of PLA. The hybridization of ZnO with $CaCO_3$ and TiO_2 did not improve the heat release properties of PLA, as these hybrids exhibited the highest PHRR and THR values. These observations indicate that combining ZnO with these inorganic fillers was ineffective in improving the flame retardancy of PLA. Figure 5c illustrates the carbon dioxide (CO_2) production profiles of the prepared composites. It is observed that the incorporation of the inorganic fillers, either individually or in combination, did not effectively suppress CO_2 production during combustion. Overall, the ZnO-based PLA composites exhibited reduced thermal stability and higher PHRR, indicating poor fire performance.

3. Materials and Methods

3.1. Materials

PLA used in this study was supplied by 2MBio Polymers, Chennai, India. It had a melt-flow index of 3 g/min and a density of 1.23 g·cm^{-3}. ZnO, TiO_2, and $CaCO_3$ were purchased from Sigma-Aldrich, Johannesburg, South Africa. ZnO had a particle size and surface area of <100 nm and 10–25 m^2·g^{-1}, respectively. Titanium (IV) oxide (TiO_2) had a particle size, surface area, and density of 21 nm, 35–65 m^2·g^{-1}, and 4.26 g·mL^{-1} at 25 °C. Calcium carbonate had a particle size of ≤30 µm and a density of 2.93 g·mL^{-1} at 25 °C.

3.2. Preparation Method

Before compounding, PLA, $CaCO_3$, ZnO, and TiO_2 were dried at 60 °C in a vacuum oven for over 12 h. The sample designations and compositions are detailed in Table 4. Neat PLA, PLA/$CaCO_3$ blend, and PLA blend composites were melt-processed using a TE-30 Co-rotating twin-screw extruder (Nanjing Only Extrusion Machinery Co., Ltd., Nanjing, China). The temperatures of the heating zones from the hopper to the die ranged from 120 °C to 180 °C. The extrusion speed was set at 178.8 rpm, and the feed rate was 4.4 kg·h^{-1}. The extrudates were quenched in water, pelletized, and then dried in an oven at 60 °C for 24 h.

Table 4. Summarized sample names and compositions.

Samples	PLA (wt.%)	Inorganic Filler (wt.%)
PLA	100	-
PLA/ZnO	97	3.0
PLA/TiO_2	97	3.0
PLA/$CaCO_3$	97	3.0
PLA/ ZnO/TiO_2	97	1.5/1.5
PLA/ZnO/$CaCO_3$	97	1.5/1.5

3.3. Characterization

The morphology of the cryo-fractured surfaces was determined using scanning electron microscopy (SEM) (Shimadzu ZU SSX 550 Superscan SEM, Kyoto, Japan) operated at a voltage of 5 kV. The samples were dipped in liquid nitrogen, then sputter-coated with carbon to reduce charging. The thermal stabilities of the samples were determined by a thermogravimetric analyzer (TGA) (model Q500, TA Instruments, Newcastle, DE, USA). Samples weighing 8–10 mg were heated at a heating rate of 10 °C·min^{-1} to 800 °C under a nitrogen atmosphere. Differential scanning calorimetry (DSC) (DSC-2500, TA Instruments, Newcastle, DE, USA) was used to determine the thermal properties and degree of crys-

tallinity of the prepared samples. Samples weighing approximately 6 mg were heated from −60 °C to 200 °C at a heating rate of 10 °C·min^{-1}, followed by cooling to −60 °C at the same rate, and then re-heated to 200 °C at 10 °C·min^{-1} in a nitrogen atmosphere with a flow rate of 50 mL·min^{-1}. The flow properties were determined using the Modula Compact Rheometer (MCR 302, Anton Paar, Graz, Austria). A 25 mm diameter parallel-plate configuration was utilized for the tests, which were conducted at 180 °C under atmospheric conditions. Preliminary experiments identified the linear viscoelastic region of the samples, and the strain amplitude was set at 1%. The zero-gap was maintained at 1.1 mm for all tests, and experiments were repeated to ensure reproducibility. The mechanical properties were determined using an Instron 5966 tester (Instron Engineering Corporation, Norwood, MA, USA), equipped with a 10 kN load cell. The tests were carried out in tension mode at a strain rate of 50 mm·min^{-1} at room temperature. Charpy impact strength was determined using CEAST Pendulum Resil Impactor II (Italy). CEAST Automatic Notchvis Plus, (Pianezza, Italy) was used to notch the samples to 2 m depth before testing. Flammability properties (heat release rate (HRR), total heat release (THR), and carbon dioxide (CO_2)) were determined using cone calorimetry (Fire Testing Technology, East Grinstead, UK). The prepared samples with the dimensions (100 × 100 × 6 mm^2) were wrapped in aluminum foil with the top surface open and exposed to the radiant cone at a heat flux of 35 kW·m^{-2}.

4. Conclusions

In this study, the effects of ZnO, TiO_2, and $CaCO_3$ as individual fillers, as well as ZnO/TiO_2 and ZnO/$CaCO_3$ hybrid fillers, on the properties of PLA were investigated. In general, ZnO can adversely affect the properties of polymers such as PLA, as observed in this study. The results demonstrated that incorporating 3 wt.% ZnO into PLA reduced its thermal stability, tensile strength, and complex viscosity while increasing the PHRR. These findings suggest that the incorporation of ZnO as a single filler may be disadvantageous for PLA, particularly when considering melt processing. When combined with TiO_2 and $CaCO_3$ at 3 wt.% (1.5 wt.% of each filler), the tensile properties and impact resistance were maintained. In addition, incorporating TiO_2 as a single filler preserved the thermal stability and tensile properties of PLA. Overall, the findings suggest that combining ZnO and TiO_2 or $CaCO_3$ may be a promising strategy for mitigating some of the adverse effects associated with ZnO incorporation into PLA during melt processing.

Author Contributions: Conceptualization, N.J., N.J.M., M.P.M. and M.J.M.; methodology, N.J., N.J.M., M.P.M. and M.J.M.; software, N.J. and M.P.M.; validation, N.J., N.J.M., M.P.M. and M.J.M.; formal analysis, N.J. and M.P.M.; investigation, N.J. and M.P.M.; resources, N.J.M. and M.J.M.; data curation, N.J., N.J.M., M.P.M. and M.J.M.; writing—original draft preparation, N.J. and M.P.M.; writing—review and editing, M.P.M., N.J.M. and M.J.M.; visualization, N.J.M. and M.J.M.; supervision, N.J.M. and M.J.M.; project administration, N.J.M. and M.J.M.; funding acquisition, N.J.M. and M.J.M. All authors have read and agreed to the published version of the manuscript.

Funding: This research received no external funding.

Institutional Review Board Statement: Not applicable.

Informed Consent Statement: Not applicable.

Data Availability Statement: The raw data supporting the conclusions of this article will be made available by the authors on request.

Conflicts of Interest: The authors declare no conflict of interest.

References

1. Wi, J.; Choi, J.; Lee, S.-H. PLA-Based Biodegradable Polymer from Synthesis to the Application. *Polymers* **2025**, *18*, 121. [CrossRef] [PubMed]
2. Chu, Z.; Zhao, T.; Li, L.; Fan, J.; Qin, Y. Characterization of Antimicrobial Poly (Lactic Acid)/Nano-Composite Films with Silver and Zinc Oxide Nanoparticles. *Materials* **2017**, *10*, 659. [CrossRef] [PubMed]
3. Demchenko, V.; Mamunya, Y.; Kobylinskyi, S.; Riabov, S.; Naumenko, K.; Zahorodnia, S.; Povnitsa, O.; Rybalchenko, N.; Iurzhenko, M.; Adamus, G.; et al. Structure-Morphology-Antimicrobial and Antiviral Activity Relationship in Silver-Containing Nanocomposites Based on Polylactide. *Molecules* **2022**, *27*, 3769. [CrossRef] [PubMed]
4. Kim, I.; Viswanathan, K.; Kasi, G.; Sadeghi, K.; Thanakkasaranee, S.; Seo, J. Poly (Lactic Acid)/ZnO Bionanocomposite Films with Positively Charged ZnO as Potential Antimicrobial Food Packaging Materials. *Polymers* **2019**, *11*, 1427. [CrossRef] [PubMed]
5. Des, S.; Mohanty, D.L.; Divya, N.; Bakshi, V.; Mohanty, A.; Rath, D.; Das, S.; Mondal, A.; Roy, S.; Sabui, R.A. Critical Review on Zinc Oxide Nanoparticles: Synthesis, Properties and Biomedical Applications. *Intell. Pharm.* **2024**, *3*, 53–70. [CrossRef]
6. Sirelkhatim, A.; Mahmud, S.; Seeni, A.; Kaus, N.H.M.; Ann, L.C.; Bakhori, S.K.M.; Hasan, H.; Mohamad, D. Review on Zinc Oxide Nanoparticles: Antibacterial Activity and Toxicity Mechanism. *Nano-Micro Lett.* **2015**, *7*, 219–242. [CrossRef] [PubMed]
7. Salaris, V.; García-Obregón, I.S.F.; López, D.; Peponi, L. Fabrication of PLA-based Electrospun Nanofibers Reinforced with ZnO Nanoparticles and In Vitro Degradation Study. *Nanomaterials* **2023**, *13*, 2236. [CrossRef] [PubMed]
8. Shojaeiarani, J.; Bajwa, D.; Jiang, L.; Liaw, J.; Hartman, K. Insight on the Influence of Nano Zinc Oxide on the Thermal, Dynamic Mechanical, and Flow Characteristics of Poly(Lactic Acid)—Zinc Oxide Composites. *Polym. Eng. Sci.* **2019**, *59*, 1242–1249. [CrossRef]
9. Morici, E.; Pecoraro, G.; Carroccio, S.C.; Bruno, E.; Scarfato, P.; Filippone, G.; Dintcheva, N.T. Understanding the Effects of Adding Metal Oxides to Polylactic Acid and Polylactic Acid Blends on Mechanical and Rheological Behaviour, We Ability, and Photo-Oxidation Resistance. *Polymers* **2024**, *16*, 922. [CrossRef] [PubMed]
10. Salehiyan, R.; Soleymani Eil Bakhtiari, S. A Review on Rheological Approaches as a Perfect Tool to Monitor Thermal Degradation of Biodegradable Polymers. *Korea-Aust. Rheol. J.* **2024**, *36*, 295–317. [CrossRef]
11. Kaseem, M.; Hamad, K.; Ur Rehman, Z. Review of Recent Advances in Polylactic Acid/TiO_2 Composites. *Materials* **2019**, *12*, 3659. [CrossRef] [PubMed]
12. Feng, S.; Zhang, F.; Ahmed, S.; Liu, Y. Physico-Mechanical and Antibacterial Properties of PLA/TiO_2 Composite Materials Synthesized via Electrospinning and Solution Casting Processes. *Coatings* **2019**, *9*, 525. [CrossRef]
13. Zhuang, W.; Liu, J.; Zhang, J.H.; Hu, B.X.; Shen, J. Preparation Characterization and Properties of TiO_2/PLA Nanocomposites by In Situ Polymerization. *Polym. Compos.* **2009**, *30*, 1074–1080. [CrossRef]
14. Baek, N.; Kim, Y.T.; Marcy, J.E.; Duncan, S.E.; O'Keefe, S.F. Physical Properties of Nanocomposite Polylactic Acid Films Prepared with Oleic Acid Modified Titanium Dioxide. *Food Packag. Shelf Life* **2018**, *17*, 30–38. [CrossRef]
15. Zárybnická, L.; Ševčík, R.; Pokorný, J.; Machová, D.; Stránská, E.; Šál, J. $CaCO_3$ Polymorphs Used as Additives in Filament Production for 3D Printing. *Polymers* **2022**, *14*, 199. [CrossRef] [PubMed]
16. Adeosun, S.O.; Usman, M.A.; Akpan, E.I.; Dibie, W.I. Characterization of LDPE Reinforced with Calcium Carbonate—Fly Ash Hybrid Filler. *J. Miner. Mater. Charact. Eng.* **2014**, *2*, 334–345. [CrossRef]
17. Chafidz, A.; Kaavessina, M.; Al-Zahrani, S.; Al-Otaibi, M.N. Rheological and Mechanical Properties of Polypropylene/Calcium Carbonate Nanocomposites Prepared from Masterbatch. *J. Thermoplast. Compos. Mater.* **2016**, *29*, 593–622. [CrossRef]
18. Shelesh-Nezhad, K.; Orang, H.; Motallebi, M. Crystallization, Shrinkage and Mechanical Characteristics of Polypropylene/CaCO3 Nanocomposites. *J. Thermoplast. Compos. Mater.* **2013**, *26*, 544–554. [CrossRef]
19. Öksüz, M.; Yildirim, H. Effect of Calcium Carbonate on the Mechanical and Thermal Proeprties of Isotactic Polypropylene/Ethylene Vinyl Acetate Blends. *J. Appl. Polym. Sci.* **2005**, *96*, 1126–1137. [CrossRef]
20. Tajdari, A.; Babaei, A.; Goudarzi, A.; Partovi, R. Preparation and study on the optical, mechanical, and antibacterial properties of polylactic acid/ZnO/TiO_2 shared nanocomposites. *J. Plast. Film Sheeting* **2020**, *36*, 285–311. [CrossRef]
21. Suntako, R. Effect of $CaCO_3$ Nanoparticles and Synthesized ZnO Nanoparticles on the Properties of Natural Rubber. *J. Phys. Conf. Ser.* **2018**, *1144*, 012156. [CrossRef]
22. Taha, E.O.; Shoaib, E.; Ahmed, M.A.; El-Ghazawy, R.A.; Naguib, H.M. Smart Biodegradable PLA Nanocomposites Reinforced with ZnO and GO for Thermomechanical and Shape Memory Applications. *Discov. Mater.* **2026**, *6*, 131. [CrossRef]
23. Wang, X.J.; Huang, Z.; Wei, M.Y.; Lu, T.; Nong, D.D.; Zhao, J.X.; Gao, X.Y.; Teng, L.J. Catalytic Effect of Nanosized ZnO and TiO2 on Thermal Degradation of Poly(Lactic Acid) and Isoconversional Kinetic Analysis. *Thermochim. Acta* **2019**, *672*, 14–24. [CrossRef]
24. Kim, H.-S.; Park, B.H.; Choi, J.H.; Yoon, J.-S. Mechanical Properties and Thermal Stability of Poly(L-lactide)/Calcium Carbonate Composites. *J. Appl. Polym. Sci.* **2008**, *109*, 3087–3092. [CrossRef]
25. Cong, Y.; Zhou, Y.; Bao, J.; Zhang, X. Crystallization, recrystallization and melting behaviors in supramolecular poly (l-lactic acid) bonded by metal-ligand coordination. *Polymer* **2024**, *294*, 126702. [CrossRef]

26. Rafaa, Z.; Boutaous, M.; Xin, S.; Siginer, D.A. Thermophysical Analysis and Modeling of the Crystallization and Melting Behavior of PLA with Talc. *J. Therm. Anal. Calorim.* **2017**, *128*, 687–698. [CrossRef]
27. Shankar, S.; Wang, L.F.; Rhim, J.W. Incorporation of Zinc Oxide Nanoparticles Improved the Mechanical, Water Vapor Barrier, UV-Light Barrier, and Antibacterial Properties of PLA-Based Nanocomposite Films. *Mater. Sci. Eng. C* **2018**, *93*, 289–298. [CrossRef] [PubMed]

Disclaimer/Publisher's Note: The statements, opinions and data contained in all publications are solely those of the individual author(s) and contributor(s) and not of MDPI and/or the editor(s). MDPI and/or the editor(s) disclaim responsibility for any injury to people or property resulting from any ideas, methods, instructions or products referred to in the content.